DOI: 10.22034/ijicmes.2025.555040.1005

University of Hormozgan

International Journal of
Innovative Computational Methods
in Engineering Sciences
*2025, * (*), *-***
journal homepage – cme.hormozgan.ac.ir

Investigation of the Effect of Fluid Field on the Vibrations of a Curved Microbeam Based on Nonclassical Continuum Mechanics under Elastic Supports

Alireza Pourmoayed[1, *], Keramat Malekzadeh Fard[2] and Roozbeh Mahmoudi[3]

[1]*Faculty of Mechanical Engineering, Khatam al-Anbiya University of Air Defense, Tehran, Iran*

[2]*Faculty of Aerospace Engineering, Malek Ashtar University of Technology, Tehran, Iran*

[3]*Islamic Azad University, Shiraz Branch, Shiraz, Iran*

ARTICLE INFO

Keywords:
Microbeam; Mechanical stability; Fluid–structure interaction; Nonlocal couple stress theory; Natural frequency; Elastic Supports

Received:
Revised:
Accepted:
Available online

ABSTRACT

Microbeams play a crucial role in mechanical processes and in the design of micro- and nanoscale structures. In many engineering applications, these structures are supported by elastic foundations, which can significantly affect their vibrational and stability characteristics. When subjected to external loading and internal fluid flow, the interaction between the microbeam and its elastic support must be accurately modeled to predict realistic dynamic behavior. The mechanical stability analysis of such structures, especially in the presence of internal fluid flow, is of great significance .In this study, the stability of a curved microbeam resting on an elastic foundation and containing an internal fluid flow is investigated. To account for the nanoscale effects, the nonlocal couple stress theory is employed for the solid domain, while the modified velocity theory is adopted for the fluid part. The internal fluid flow is analyzed using the Navier–Stokes equations, and the governing equations of the microbeam are derived from Hamilton's principle. The fluid–structure interaction is modeled as a two-way coupled phenomenon. The governing differential equations are solved numerically using the Galerkin method combined with Gauss quadrature integration .The results reveal that size effects play a significant role in the stability analysis and neglecting nonclassical continuum mechanics may result in considerable errors. Small curvatures are found to have a noticeable influence on the vibrational behavior of the microbeam system. Increasing the fluid flow velocity enhances system instability and reduces the natural frequency. Furthermore, the type of fluid and the stiffness of the elastic foundation have a remarkable impact on the system's dynamic response. Overall, this study demonstrates that accurate mechanical modeling of microbeams, incorporating both size-dependent effects and elastic foundation interactions, can provide valuable insights for the design and optimization of micro- and nanoscale structures.

1. Introduction

Carbon nanotubes (CNTs) and other nanostructures, due to their unique nanoscale properties, have found extensive applications in various engineering fields such as nanosensors, nanocomposites, and nanorobotics. The mechanical behavior of nanotubes is influenced by several factors, including material properties, boundary conditions, and different working environments [1–3]. One of the key aspects in analyzing the dynamic behavior and stability of nanotubes is the fluid–structure interaction, which must be taken into

* Corresponding author. e-mail: a.pourmoayed@khadu.ac.ir

account when studying such systems. Fluid-conveying tubes are of particular importance due to their widespread applications in diverse industries, including mechanical and aerospace engineering, nanotechnology, and the oil and gas industry. These tubes behave as dynamic structures subjected to both internal forces generated by the internal fluid flow and external mechanical loads. When fluid flows inside such tubes, the interaction between the fluid and the tube wall can lead to mechanical instabilities such as vibrations, divergence, and flutter phenomena. These effects can significantly influence the performance of the tube and may even result in structural failure [4–5]. One of the main challenges in studying nanotubes lies in accurately accounting for size effects in mechanical analyses. Classical elasticity theory alone is insufficient for modeling these effects at the nanoscale. Therefore, advanced continuum theories such as the nonlocal elasticity theory and the couple stress theory have been developed to better describe the mechanical behavior of nanostructures. The nonlocal theory suggests that the mechanical properties of materials at the nanoscale depend not only on the immediate neighborhood of a point but also on the influence of more distant points. This theory introduces parameters known as nonlocal parameters, which capture the long-range atomic interactions and generally predict the softening behavior of materials at small scales.

On the other hand, the couple stress theory provides a more refined description of material behavior by incorporating the effects of internal rotations and couple moments within the continuum. This theory is particularly useful for analyzing nanotubes and can predict material stiffening phenomena at the nanoscale [6–10]. In the dynamic analysis of nanotubes conveying fluid, one of the critical parameters is the size effect, which strongly affects their vibrational and stability characteristics. Recent studies have shown that in nanoscale gas and liquid flows, nonlocal and couple-stress parameters can significantly modify the dynamic response of nanotubes [11–12]. In the present study, the main objective is to investigate the dynamic behavior of fluid-conveying nanotubes and to examine the influence of curvature effects using a combined nonlocal and couple stress theoretical framework. This analysis focuses on fluid–structure interaction phenomena in nanotubes and aims to provide valuable insights for improving the design and performance of such structures in various nanoscale applications.

2. Theoretical Formulation and methodology

In this study, the frequency analysis of a microbeam with a circular cross-section of radius R and length L, incorporating local curvatures in its structure, is investigated under the effects of internal fluid flow and an external viscoelastic force. At the final stage of this research, the influence of the internal fluid flow on the stability of the microbeam will be examined. A schematic representation of the problem is illustrated in the figure below.

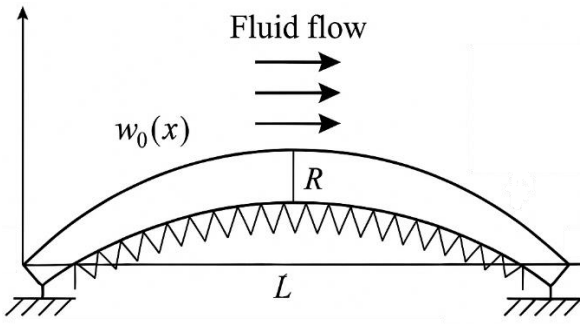

Figure 1. Schematic representation of the problem.

Considering that the length-to-radius ratio of the microbeam is relatively high, the Euler–Bernoulli beam theory provides an appropriate assumption for the present analysis. According to this theory, the displacement components can be expressed as follows:

$$u_x = u_{(x,t)} - z\frac{\partial w}{\partial x} \tag{1}$$

$$u_y = 0 \tag{2}$$

$$u_z = w_{(x.t)} + w_0 \tag{3}$$

The symbols u_x, u_y and u_z denote the displacement components along the x, y, and z directions, respectively. The terms u and w represent the displacements of the neutral axis in the x and z directions, respectively, while w_0 denotes the initial curvature of the microbeam, which is defined as follows:

$$w_0 = A_0 \operatorname{Sin}\left(\frac{\pi x}{L}\right) \tag{4}$$

The strain field can be obtained using the strain–displacement relations together with the displacement field of the Euler–Bernoulli beam theory. The nonlinear strains are expressed as follows:

$$\varepsilon_{xx} = \frac{\partial u}{\partial x} + \frac{1}{2}\left(\frac{\partial w}{\partial x}\right)^2 - z\frac{\partial^2 w}{\partial x^2} + \frac{\partial w}{\partial x}\frac{\partial w_0}{\partial x} \tag{5}$$

The term ε_{xx} represents the normal strain in the x. All other strain components vanish due to the assumed displacement field. To incorporate the nonlinear geometric effects, the von Kármán nonlinear term is added to the strain field. The rotation term can be obtained from the displacement field as follows:

$$\chi_{xy} = -\frac{1}{2}\left[\frac{\partial^2 w}{\partial x^2} + \frac{1}{2}\frac{\partial^2 w_0}{\partial x^2}\right] \tag{6}$$

In this study, both the couple stress theory and the nonlocal elasticity theory are employed simultaneously. The couple stress theory predicts stiffening effects at the nanoscale; in other words, the responses obtained from this theory exhibit higher stiffness compared with those of the classical elasticity theory. Conversely, the nonlocal elasticity theory predicts softening behavior, as it considers the long-range interactions between atoms and reduces the overall stiffness of the material. Since, under different physical conditions, both stiffening and softening behaviors may occur simultaneously, in the present analysis a combined nonlocal–couple stress model is adopted. The constitutive relation combining the effects of both the nonlocal elasticity and the couple stress theories is expressed as follows:

$$\sigma_{xx} - \mu^2 \frac{\partial^2 \sigma_{xx}}{\partial x^2} = \mathrm{E}\varepsilon_{xx} \tag{7}$$

$$m_{xy} - \mu^2 \frac{\partial^2 m_{xy}}{\partial x^2} = 2GL^2 . \chi_{xy} \tag{8}$$

To derive the displacement equations of elastic materials, several methods can be employed, such as Newton's equations of motion, energy methods, the principle of virtual work, minimization of the total potential energy, and Hamilton's principle. In this study, Hamilton's principle is utilized to obtain the governing equations of the problem.

$$\int_0^t \left(\delta U + \delta W - \delta K\right) dt = 0 \tag{9}$$

where δ denotes the variation operator, and U, W, and K represent the strain energy, the work done by external forces, and the kinetic energy, respectively.

By combining the above relations and applying the integration by parts, the equations of motion of the microbeam subjected to the external fluid force and local curvature can be obtained as follows:

$$\frac{\partial N_{xx}}{\partial x} = 0 \tag{10}$$

$$\frac{\partial}{\partial x}\left(N_{xx}\left(\frac{\partial w}{\partial x} + \frac{dw_0}{dx}\right)\right) - \frac{\partial^2}{\partial x^2}\left(M_{xx} + Y_{xy}\right) + \rho I \frac{\partial^4 w}{\partial x^2 \partial t^2} - \rho A \frac{\partial^2 w}{\partial t^2} - F_{ext} = 0 \tag{11}$$

where I denotes the area moment of inertia, which is defined as follows:

$$I = \int_A z^2 dA \tag{12}$$

By combining the constitutive relations with the equations of motion of the microbeam, the governing Navier equation for the problem is obtained as follows:

$$-\left[F_{ext} - N_{xx}\left(\frac{\partial^2 w}{\partial x^2} + \frac{d^2 w_0}{dx^2}\right) + \rho A \frac{\partial^2 w}{\partial t^2} - \rho I \frac{\partial^4 w}{\partial x^2 \partial t^2}\right] + \mu^2 \begin{bmatrix} \frac{\partial^2 F_{ext}}{\partial x^2} - N_{xx}\left(\frac{\partial^4 w}{\partial x^4} + \frac{d^4 w_0}{dx^4}\right) \\ +\rho A \frac{\partial^4 w}{\partial x^4 \partial t^2} - \rho I \frac{\partial^6 w}{\partial x^4 \partial t^2} \end{bmatrix}$$
$$= -GL^2 A\left[\frac{\partial^4 w}{\partial x^4}\right] - \frac{1}{2} GL^2 A\left[\frac{d^4 w_0}{dx^4}\right] - EI \frac{\partial^4 w}{\partial x^4} \tag{13}$$

In the above equation, F_{ext} represents the force exerted on the system by the fluid flowing inside the microbeam. The velocity field of the fluid flow inside the microbeam is introduced as follows:

$$v = v_x(r)\hat{e}_x + v_r(x,t)\hat{e}_r \tag{14}$$

To satisfy the fluid–structure interaction, the following equation must be fulfilled:

$$v_r(x,t) = \frac{Dw}{Dt} \tag{15}$$

Here, V_x denotes the mean flow velocity in the direction of the fluid flow. The external force acting on the microbeam corresponds to the pressure variation in the direction normal to the flow. To obtain this force, the Navier–Stokes equation is written in the r-direction, assuming a fully developed

$$\frac{\partial p}{\partial r} = \mu\left[\frac{\partial^3 w}{\partial x^2 \partial t} + \bar{v}_x \frac{\partial^3 w}{\partial x^3}\right]$$
$$-\rho\left[\frac{\partial^2 w}{\partial t^2} + 2\bar{v}_x \frac{\partial^2 w}{\partial x \partial t} + \bar{v}_x^2 \frac{\partial^2 w}{\partial x^2}\right] \tag{16}$$

Since the viscous term is negligible, it can be safely ignored in the analysis.

$$f_1 = -m_f\left[\frac{\partial^2 w}{\partial t^2} + 2\bar{v}_x \frac{\partial^2 w}{\partial x \partial t} + \bar{v}_x^2 \frac{\partial^2 w}{\partial x^2}\right] \tag{17}$$

Here, m denotes the mass of the fluid per unit length, and A represents the cross-sectional area of the internal fluid. The behavior of fluid flow at the nanoscale differs significantly from that at larger scales, particularly at low Reynolds numbers. Therefore, for the present problem, the no-slip boundary condition between the fluid and the microbeam wall cannot be applied. Instead, the Velocity Correction Factor (VCF) proposed by *Rashidi et al.* is employed, which incorporates both the size effects and the slip boundary condition in the flow analysis.

$$VCF = \frac{\bar{V}_X}{U} = (1 + \alpha' Kn)(4(\frac{2 - \sigma_V}{\sigma_V})(\frac{Kn}{1 + Kn}) + 1) \tag{18}$$

Here, $\bar{v}_x$ and U denote the average flow velocities inside the microbeam, where $\bar{V}_x$ satisfies the slip boundary condition, while U corresponds to the case without slip effects. Kn represents the Knudsen number, σ_V is the tangential momentum accommodation coefficient, and α' is a coefficient that depends on the Knudsen number. According to the investigations conducted by *Rashidi et al.*, the numerical value of σ_V is taken as 0.7.

$$\alpha' = \alpha_0 \frac{2}{\pi}\left(\tan^{-1}(\alpha_1 Kn^B\right) \tag{19}$$

In the above relation, α_1 and B are empirical parameters, and α_0 is defined as follows:

$$\alpha_0 = \frac{64}{3\pi(1-\frac{4}{b})} \tag{20}$$

For the second-order slip boundary condition, the parameter b is set to 1. In the study of fluid flow at the nanoscale, the Knudsen number (Kn) must be evaluated, which is defined as the ratio of the molecular mean free path to the characteristic length (or diameter) of the nanoparticle. It can be used as a distinguishing factor to account for small-scale (size-dependent) effects in the flow field. According to *Knudsen*, the fluid flow can be categorized into four regimes based on the value of Kn :

1. Continuum flow regime ($Kn < 10^{-3}$)
2. Slip flow regime ($10^{-3} < Kn < 10^{-1}$)
3. Transition flow regime ($10^{-1} < Kn < 10$)
4. Free molecular flow regime ($Kn > 10$)

$$F_{ext} = f_1 + f_2$$

$$f_1 = -m_f\left[\frac{\partial^2 w}{\partial t^2} + 2(VCF)U\frac{\partial^2 w}{\partial x \partial t} + (VCF)^2 U^2 \frac{\partial^2 w}{\partial x^2}\right]$$

$$f_2 = -k_1 w \tag{21}$$

By considering the small-scale effects in the fluid flow, the above equation can be rewritten accordingly. By substituting the external force field into Eq. (13), the governing Navier equation of the problem can be expressed as follows:

$$-\begin{bmatrix} -k_1 w - m_f\left[\frac{\partial^2 w}{\partial t^2} + 2(VCF)U\frac{\partial^2 w}{\partial x \partial t} + (VCF)^2 U^2 \frac{\partial^2 w}{\partial x^2}\right] \\ -N_{xx}\left(\frac{\partial^2 w}{\partial x^2} + \frac{d^2 w_0}{dx^2}\right) + \rho A \frac{\partial^2 w}{\partial t^2} - \rho I \frac{\partial^4 w}{\partial x^2 \partial t^2} \end{bmatrix} + \mu^2 \begin{bmatrix} \frac{\partial^2 F_{ext}}{\partial x^2} - N_{xx}\left(\frac{\partial^4 w}{\partial x^4} + \frac{d^4 w_0}{dx^4}\right) \\ +\rho A \frac{\partial^4 w}{\partial x^4 \partial t^2} - \rho I \frac{\partial^6 w}{\partial x^4 \partial t^2} \end{bmatrix}$$

$$= -GL^2 A\left[\frac{\partial^4 w}{\partial x^4}\right] - \frac{1}{2}GL^2 A\left[\frac{d^4 w_0}{dx^4}\right] - EI\frac{\partial^4 w}{\partial x^4} \tag{22}$$

The non-dimensional form of Eq. (22) can be expressed as follows:

$$B\frac{\partial^2 \overline{w}}{\partial \tau^2} + 2B^{\frac{1}{2}}(VCF).\bar{U}\frac{\partial^2 \overline{w}}{\partial \overline{x}.\partial \tau} + VCF^2.\bar{U}^2\frac{\partial^2 \overline{w}}{\partial \overline{x}^2} + \bar{k}_1 \overline{w} + \left(\frac{1}{2\bar{I}}\int_0^L \frac{\partial \overline{w}}{\partial \overline{x}} d\overline{x} - \frac{1}{\bar{I}}\int_0^L \frac{\partial \overline{w}}{\partial \overline{x}}.\frac{\partial w_0}{\partial \overline{x}} d\overline{x}\right)\left(\frac{\partial^2 w}{\partial \overline{x}^2}.\frac{\partial^2 \overline{w}_0}{\partial \overline{x}^2}\right)$$

$$-\frac{\partial^2 \overline{w}}{\partial \tau^2} - \bar{I}\frac{\partial^4 \overline{w}}{\partial \overline{x}^2 \partial \tau^2} + \bar{\mu}^2 B\frac{\partial^4 \overline{w}}{\partial \overline{x}^2.\partial \tau^2} - 2\bar{\mu}^2.VCF.\bar{U}.B\frac{\partial^4 \overline{w}}{\partial \overline{x}^3 \partial \tau} - VCF^2.\bar{U}^2.\bar{\mu}^2\frac{\partial^4 \overline{w}}{\partial \overline{x}^4} + \bar{k}_1\frac{\partial^2 \overline{w}}{\partial \overline{x}^2}$$

$$(\frac{1}{2\bar{\tau}}\int_0^L (\frac{\partial \overline{w}}{\partial \overline{x}})^2 d\overline{x} - \frac{1}{\bar{I}}\int_0^L \frac{\partial \overline{w}}{\partial \overline{x}}\frac{\partial \overline{w}_0}{\partial \overline{x}} d\overline{x})\bar{\mu}^2\frac{\partial^4 \overline{w}}{\partial \overline{x}^4}\frac{\partial^4 \overline{w}_0}{\partial \overline{x}^4} - \bar{\mu}^2\frac{\partial^4 \overline{w}}{\partial \overline{x}^2 \partial \tau^2} + \bar{\mu}^2\frac{1}{\bar{I}}\frac{\partial^6 \overline{w}}{\partial \overline{x}^4 \partial \tau^2}$$

$$= \frac{1}{2(1+\nu)}\frac{1}{\bar{I}}\bar{l}^2\frac{\partial^4 \overline{w}}{\partial \overline{x}^4} - \frac{1}{2}\frac{1}{2(1+\nu)}\bar{l}\frac{1}{\bar{I}}\frac{\partial^4 w_0}{\partial \overline{x}^4} - \frac{\partial^4 \overline{w}}{\partial \overline{x}^4} \tag{23}$$

The following non-dimensional parameters are used Eq. (22):

$$\bar{\mu}=\frac{\mu}{L},\bar{l}=\frac{l}{L},G=\frac{E}{2(1+\upsilon)},U=\bar{U}\left(\frac{E\mathrm{I}}{m_f}\right)^{\frac{1}{2}}\frac{1}{L}$$

$$s=\frac{1}{2(1+\upsilon)},B=\frac{m_f}{pA} \tag{24}$$

The governing Navier equation of the problem is solved using the semi-analytical Galerkin method. For applying the Galerkin method, the formulation is defined as follows:

$$R=B\frac{\partial^2\tilde{w}}{\partial\tau^2}+2B^{\frac{1}{2}}(VCF).\bar{U}\frac{\partial^2\tilde{w}}{\partial\bar{x}.\partial\tau}+VCF^2.\bar{U}^2\frac{\partial^2\tilde{w}}{\partial\bar{x}^2}+\bar{k}_1\bar{w}+\bar{k}_1\frac{\partial^2\bar{w}}{\partial\bar{x}^2}$$

$$\left(\frac{1}{2\bar{I}}\int_0^L\frac{\partial\tilde{w}}{\partial\bar{x}}d\bar{x}-\frac{1}{\bar{I}}\int_0^L\frac{\partial\tilde{w}}{\partial\bar{x}}.\frac{\partial\tilde{w}_0}{\partial\bar{x}}d\bar{x}\right)\left(\frac{\partial^2\tilde{w}}{\partial\bar{x}^2}.\frac{\partial^2\tilde{w}_0}{\partial\bar{x}^2}\right)$$

$$-\frac{\partial^2\tilde{w}}{\partial\tau^2}-\bar{I}\frac{\partial^4\tilde{w}}{\partial\bar{x}^2\partial\tau^2}+\bar{\mu}^2B\frac{\partial^4\bar{w}}{\partial\bar{x}^2.\partial\tau^2}-2\bar{\mu}^2.VCF.\bar{U}.B\frac{\partial^4\tilde{w}}{\partial\bar{x}^3\partial\tau}-VCF^2.\bar{U}^2.\bar{\mu}^2\frac{\partial^4\tilde{w}}{\partial\bar{x}^4}+$$

$$(\frac{1}{2\bar{\tau}}\int_0^L(\frac{\partial\tilde{w}}{\partial\bar{x}})^2d\bar{x}-\frac{1}{\bar{I}}\int_0^L\frac{\partial\tilde{w}}{\partial\bar{x}}\frac{\partial\tilde{w}_0}{\partial\bar{x}}d\bar{x})\bar{\mu}^2\frac{\partial^4\tilde{w}}{\partial\bar{x}^4}\frac{\partial^4\tilde{w}_0}{\partial\bar{x}^4}-\bar{\mu}^2\frac{\partial^4\tilde{w}}{\partial\bar{x}^2\partial\tau^2}+\bar{\mu}^2\frac{1}{\bar{I}}\frac{\partial^6\tilde{w}}{\partial\bar{x}^4\partial\tau^2}$$

$$-\frac{1}{2(1+\nu)}\frac{1}{\bar{I}}\bar{l}^2\frac{\partial^4\tilde{w}}{\partial\bar{x}^4}+\frac{1}{2}\frac{1}{2(1+\nu)}\bar{l}\frac{1}{\bar{I}}\frac{\partial^4\tilde{w}_0}{\partial\bar{x}^4}+\frac{\partial^4\tilde{w}}{\partial\bar{x}^4} \tag{25}$$

where $\tilde{w}$ is defined as follows:

$$\tilde{w}=\sum_{i=1}^{n}\phi_i(\bar{x}).T_i(\tau) \tag{26}$$

here the function $\phi(\bar{x})$ must satisfy the geometric boundary conditions. For the pinned–pinned (simply supported) boundary condition, it is defined as follows:

$$\phi_i=\sin\frac{i\pi x}{L} \tag{27}$$

Finally, by applying the Galerkin method and eliminating the spatial dependency, the governing equation can be expressed as follows:

$$\int_0^1\phi(\bar{x})Rd\bar{x}=0 \tag{28}$$

To describe the vibrational behavior of the system, the first-mode eigenvalue is calculated using Ω. In general, Ω is a complex number consisting of both real and imaginary parts, which can be used to characterize the dynamic response and stability of the system. Based on the vibrational behavior, as the fluid flow velocity increases, the imaginary part of the first-mode eigenvalue decreases, indicating that the microbeam becomes more flexible. When the flow velocity reaches a certain critical value, the imaginary part approaches zero, which signifies the onset of instability in the system.

3. Results

To validate the results of the present study, the work of Ramezani and Mojra [11] was used for comparison. In their research, the effects of curvature and couple stress were neglected. The validation results are presented in Table 1, which clearly indicate that the outcomes of the present analysis exhibit high accuracy and an excellent agreement with the reference data.

Table 1. Comparison of the present results with previous studies

	$\overline{u}_{cr}$		
$[k_n, \bar{\mu}]$	$[0,0]$	$[0.001,0]$	$[0.001,0.2]$
Present Work	3.142	3.119	2.641
Ramezani and Mojra [11]	3.142	3.118	2.641

Figure 2 illustrates the variation of the natural frequency with respect to the fluid velocity for the maximum curvature amplitude. As shown in Figure 2, increasing the maximum curvature leads to an increase in the natural frequency. However, variations in A_0 have no noticeable effect on the critical velocity of the microbeam. The critical velocity is defined as the flow velocity at which the imaginary part of the frequency becomes zero, while the real part remains finite. For velocities higher than the critical value, the system becomes unstable, and the displacement field of the microbeam tends to diverge toward infinity. In contrast, for velocities lower than the critical value, the system exhibits oscillatory behavior and remains stable.

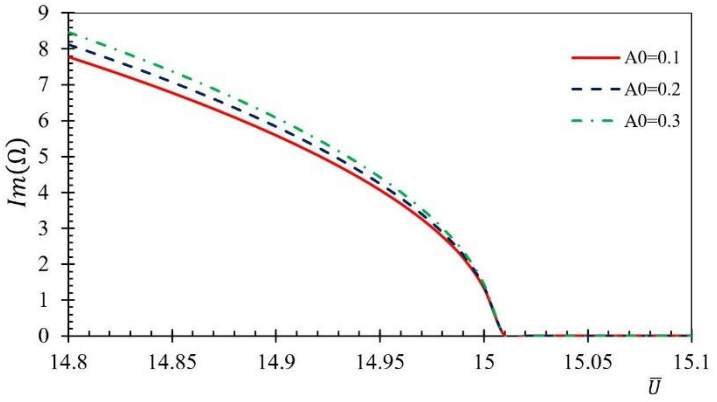

Figure 2. Effect of the maximum curvature amplitude of the microbeam on its natural frequency

Figure 3 investigates the effect of the nonlocal elasticity parameter on the critical velocity and the natural frequency of the microbeam. As the nonlocal parameter (μ) increases, the critical velocity decreases, indicating that an increase in μ leads to reduced stability of the system. As reported in the literature, an increase in the nonlocal parameter μ predicts a softening behavior, which is clearly observed in the present figure.

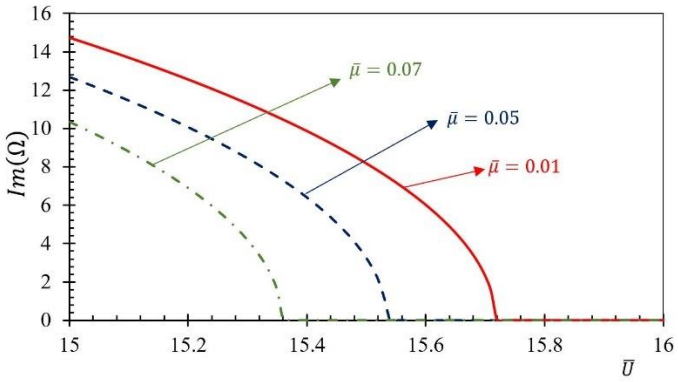

Figure 3. Influence of the nonlocal elasticity parameter on the natural frequency of the microbeam

Figure 4 investigates the effect of the couple stress length-scale parameter on the critical fluid velocity. As shown in this figure, an increase in the parameter $\bar{l}$ leads to a significant increase in the critical velocity, which indicates the presence of size effects. Neglecting these effects may lead to substantial errors in the analysis. Moreover, as the parameter $\bar{l}$ increases, the stability of the system also improves. As previously discussed, the couple stress theory predicts a stiffening behavior, and the results presented in this figure confirm that an increase in the couple stress parameter enhances both the critical velocity and the stability of the microbeam system.

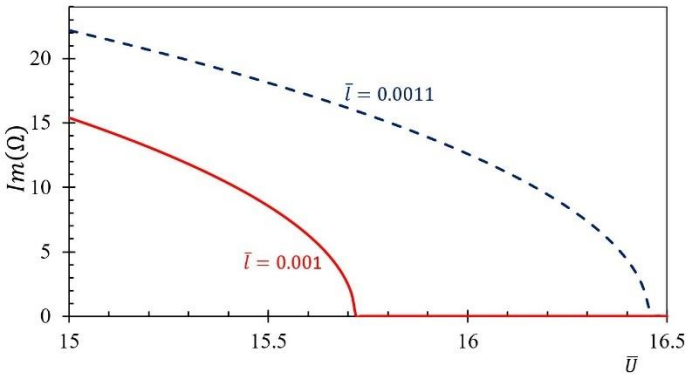

Figure 4. Influence of the couple stress length-scale parameter on the natural frequency of the microbeam

Figure 5 illustrates the variation of the natural frequency of the system with respect to the parameter β. The parameter β represents the type of fluid flowing inside the microtube; smaller values of β correspond to gaseous flows, while larger values indicate liquid flows. As shown in this figure, increasing the value of β leads to a decrease in the natural frequency, implying that the natural frequency differs depending on whether the internal fluid is a gas or a liquid.

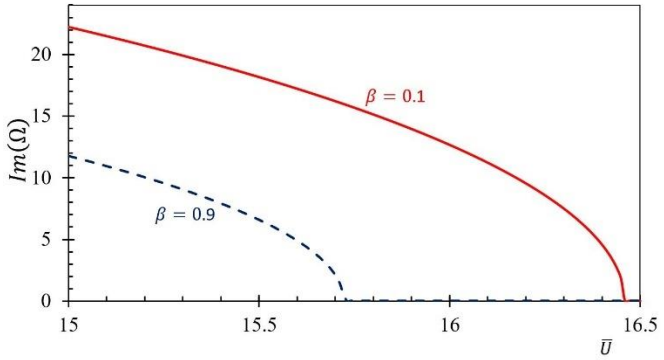

Figure 5. Influence of the fluid type on the natural frequency of the microbeam

Figure 6 illustrates the variation of the imaginary part of the natural frequency, with respect to the fluid velocity, for different values of the support stiffness parameter. As can be seen, increasing support stiffness parameter shifts the curves to the right and leads to a higher critical velocity. This indicates that a stiffer support condition enhances the stability of the system. For K1=0, where the microbeam has a softer support, instability occurs at lower velocities, whereas for higher stiffness values (K1=10 and K1=20), the system becomes more stable, and instability appears at higher flow velocities.

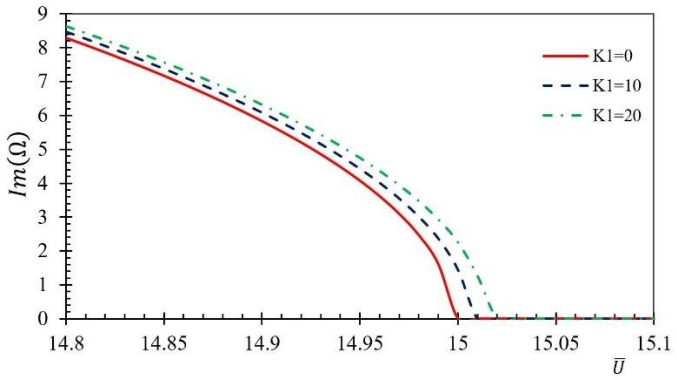

Figure 6. Effect of the support condition on the natural frequency of the microbeam

4. Conclusion

In this study, the dynamic stability and vibration behavior of a curved microbeam conveying internal fluid were investigated based on a combined nonlocal couple stress theory and modified fluid velocity model. The governing equations were derived using Hamilton's principle, and the fluid–structure interaction was considered as a two-way coupled system. The resulting nonlinear equations were solved by employing the Galerkin method and Gauss quadrature integration. The results revealed that the size effects play a crucial role in the dynamic response of microbeams. Neglecting the nonclassical continuum effects can lead to significant errors in predicting the system's stability and natural frequency. The nonlocal elasticity parameter induces a softening effect, resulting in reduced stiffness and lower critical velocity, while the couple stress parameter introduces a stiffening effect, enhancing both the critical velocity and the overall stability of the system. Furthermore, the analysis demonstrated that the maximum curvature of the microbeam significantly affects its natural frequency and increasing the fluid flow velocity decreases the natural frequency while increasing the likelihood of instability. The type of internal fluid also has a noticeable influence—systems conveying liquids exhibit lower natural frequencies compared to those conveying gases. Additionally, stiffer boundary supports were shown to delay the onset of instability and increase the critical flow velocity. Overall, the present study highlights the necessity of incorporating both nonlocal elasticity and couple stress effects in the modeling of micro- and nanoscale structures. The proposed model provides a more accurate and physically consistent framework for predicting the stability and vibrational behavior of microbeams conveying fluids, which can be valuable for the design and optimization of micro- and nano-electromechanical systems (MEMS/NEMS) and fluidic microdevices

5. References:

1. C. Li and T.-W. Chou, "A structural mechanics approach for the analysis of carbon nanotubes," *Int. J. Solids Struct*., vol. 40, no. 10, pp. 2487–2499, May 2003.
2. J. P. Salvetat, J. M. Bonard, N. H. Thomson, A. J. Kulik, L. Forro, W. Benoit, and L. Zuppiroli, "Mechanical properties of carbon nanotubes," *Appl. Phys. A*, vol. 69, pp. 255–260, 1999.
3. V. Khanna, V. Kumar, and S. A. Bansal, "Mechanical properties of aluminium-graphene/carbon nanotubes (CNTs) metal matrix composites: Advancement, opportunities and perspective," *Mater. Res. Bull*., vol. 138, pp. 111224, 2021.
4. Q. Jin and Y. Ren, "Review on mechanics of fluid-conveying nanotubes," *Int. J. Eng. Sci*., vol. 195, pp. 104007, 2024.
5. A. Farajpour, H. Farokhi, M. H. Ghayesh, and S. Hussain, "Nonlinear mechanics of nanotubes conveying fluid," *Int. J. Eng. Sci*., vol. 133, pp. 132–143, 2018.
6. M. O. Belarbi et al., "Nonlocal vibration of functionally graded nanoplates using a layerwise theory," *Math. Mech. Solids*, vol. 27, no. 12, pp. 2634–2661, 2022.
7. S. Aydinlik, A. Kiris, and W. Sumelka, "Nonlocal vibration analysis of microstretch plates in the framework of space-fractional mechanics—theory and validation," *Eur. Phys. J. Plus*, vol. 136, no. 2, pp. 1–17, 2021.

1. Q. H. Pham et al., “Modified nonlocal couple stress isogeometric approach for bending and free vibration analysis of functionally graded nanoplates,” *Eng. Comput*., vol. 39, no. 1, pp. 993–1018, 2023.
2. R. Mahmoudi, A. Barati, M. Hosseini, and A. Hadi, “Torsional vibration of functionally porous nanotube based on nonlocal couple stress theory,” *Int. J. Appl. Mech*., vol. 13, no. 10, pp. 2150122, 2021.
3. Y. Zhou, Y. F. Zheng, F. Wang, and C. P. Chen, “Size-dependent nonlinear free vibration of magneto-electro-elastic nanobeams by incorporating modified couple stress and nonlocal elasticity theory,” *Phys. Scr*., vol. 99, no. 9, pp. 095217, 2024.
4. S. R. Ramezani and A. Mojra, “Stability analysis of conveying-nanofluid CNT under magnetic field based on nonlocal couple stress theory and fluid-structure interaction,” *Mech. Based Des. Struct. Mach*., vol. 51, no. 1, pp. 583–600, 2023.
5. S. R. Ramezani and A. Mojra, “Thermal-magneto-mechanical stability analysis of nanofluid conveying carbon nanotubes based on nonlocal couple stress theory,” *J. Therm. Stresses*, vol. 44, no. 10, pp. 1221–1243, 2021.